Analysis of SAR on flat phantom for different multi-antenna mobile terminals

Li, Hui; Tsiaras, Apostolos; Derat, Benoit; Lau, Buon Kiong

Published in:
European Conference on Antennas and Propagation (EuCAP), 2014

DOI:
10.1109/EuCAP.2014.6902194

2014

Document Version:
Peer reviewed version (aka post-print)

Analysis of SAR on Flat Phantom for Different Multi-antenna Mobile Terminals

Hui Li[1], Apostolos Tsiaras[1], Benoît Derat[2], Buon Kiong Lau[1]
[1]Department of Electrical and Information Technology, Lund University, Lund, Sweden, hui.li@eit.lth.se
[2] ART-FI SAS, Orsay, France

***Abstract*— Evaluation of Specific Absorption Rate (SAR) for multiple antenna systems is becoming important, with the upcoming deployment of LTE-Advanced. In this work, the influence of different antenna locations and antenna types was investigated for stand-alone SAR and simultaneous SAR, to provide some guidelines for antenna design in multi-antenna handsets. For simultaneous SAR, different phase shifts between antenna ports were considered and the averaged SAR was used as a metrics for comparison. The SAR performances were evaluated in simulation for the body worn scenario, and different placements of the mobile handset, i.e., with either the screen or back side closer to the body, were studied.**

***Index Terms*—mobile antenna, MIMO system, SAR.**

I. INTRODUCTION

Although challenging, the implementation of multi-antennas in compact mobile terminals in Long Term Evolution (LTE) systems is necessary to reach highest possible data-rates. Multiple-input multiple-output (MIMO) technology is indeed crucial for providing the top download rates of up to 300 megabits per second (Mbps) in LTE. However, LTE focuses on improving the downlink, and does not mandate the use of multi-antennas on the uplink. This means that classical standard test procedures for evaluating human exposure to radio-frequency (RF) fields based on single-antenna systems can be applied for LTE uplink transmissions [1-3]. For exposure of the body to a RF electromagnetic field in the range of frequencies used for LTE, the metric of Specific Absorption Rate (SAR) is used and defined as the power absorbed per mass of tissue, having a unit of watt per kilogram (W/kg):

$$\mathrm{SAR} = \frac{\sigma}{2\rho}|E|^2, \qquad (1)$$

where σ and ρ denote the conductivity and mass density of the tissue, respectively. E is the induced electrical field in the biological tissue. In this paper, the SAR value measured for a single port excitation of a multi-antenna device is called stand-alone SAR. Apart from single-antenna systems, stand-alone SAR can also be used to characterize the SAR performance of each of the multi-antennas in a selection diversity scheme.

On the other hand, LTE-Advanced [4] provides different uplink MIMO schemes, including the spatial multiplexing (SM) scheme that requires simultaneous excitation of multi-antennas with different signals. SAR evaluation is more complicated for SM, since the simultaneous excitation of multi-antennas results in the near-field to vary significantly according to the phase relationship of the transmitted signals over the antenna elements.

SAR on traditional single-antenna terminals has been well studied [5-7]. However, for compact MIMO enabled terminal devices, strong mutual coupling between the antenna elements can greatly change the SAR behavior. Thus, antenna design plays an important role even for stand-alone SAR. So far, studies on SAR performance for multi-antennas are quite limited [8-10]. A technique to optimize SAR in multi-antenna systems was proposed in [9] using beamforming. In [10], SAR levels for ground free, on ground and co-located multi-antennas were investigated. The metrics of SPLSR (SAR to peak location spacing ratio) was used in evaluating and comparing simultaneous SAR for different antenna setups. However, SPLSR, which has the unit of W/kg/cm, does not strictly quantify SAR. Instead, it is only intended as a criterion to decide whether or not simultaneous SAR needs to be further investigated. Reference [10] also focused on the head phantom case. To evaluate the influence of antenna design factors (e.g., antenna location and type), it may be more intuitive to study the flat phantom (body-worn) case. This is because the phantom is geometrically uniform, which allows the study to be independent of the influence of an irregular geometry (e.g., the head).

In this context, this work aims at: 1) showing the influence of antenna locations and antenna types on stand-alone and simultaneous SAR for the flat phantom case; 2) comparing SAR behaviors when different sides of the mobile phones are facing the flat phantom, since mobile phones are usually arbitrarily inserted into the pocket in real life, either with the screen or the back side facing the body. For simultaneous SAR, phase differences between the ports were considered, and average simultaneous SAR was taken over different phase shifts (from 0° to 360°).

II. SYSTEM SETUP

Antenna setup: Two groups of antenna setups were investigated in this work. Group A consists of two handsets, with each integrated with two identical coupled-fed monopole antennas. In one handset, the antenna elements are co-located on the same short edge of the chassis, whereas the antennas are separated on different edges of the chassis in the other handset, as shown in Fig. 1 (a). Group B comprises three setups with the same antenna locations but different antenna types, i.e., dual-monopole setup, dual-PIFA setup, and monopole-and-

This work was supported in part by a Short Term Scientific Mission (STSM) grant from COST Action IC1004 (COST-STSM-IC1004-14193) and in part by Vetenskapsrådet under grants no. 2010-468 and 2012-4859.

PIFA setup, as shown in Fig. 1(b). The size of the chassis for all the antenna setups is 130 mm × 66 mm. In free space, the coupled-fed monopoles in group A cover 0.783-0.969 GHz for the low band and 1.54-2.67 GHz for the high band. In Group B, the folded monopoles cover the 0.83-0.895 GHz and 1.82-2 GHz bands, whereas the PIFAs operate at the 0.837-0.872 GHz and 1.84-1.98 GHz bands. In this paper, 1g peak spatial-average SAR is investigated at the center frequency of each band for all antenna setups: 0.859 GHz and 1.92 GHz, which also correspond to the center frequency of LTE Band 5 and Band 2, respectively.

Phantom setup: The flat phantom is composed of two parts: an inner liquid material of size 225 × 150 × 150 mm^3 and an outer shell with a thickness of 2 mm. The dielectric properties of the flat phantom at the center frequencies are presented in Table I and comply with [2]. The antennas are placed 3 mm above the flat phantom, corresponding to the worst case when the mobile handset is placed very close to the body, e.g., in a tight pocket with a very thin casing. Two sides of the mobile antennas are considered as noted in Fig. 2: side 1 refers to the case where the chassis (i.e., screen side of mobile handset) is close to the phantom, whereas side 2 refers to the case that the antenna elements (i.e., back side or battery side) face the phantom.

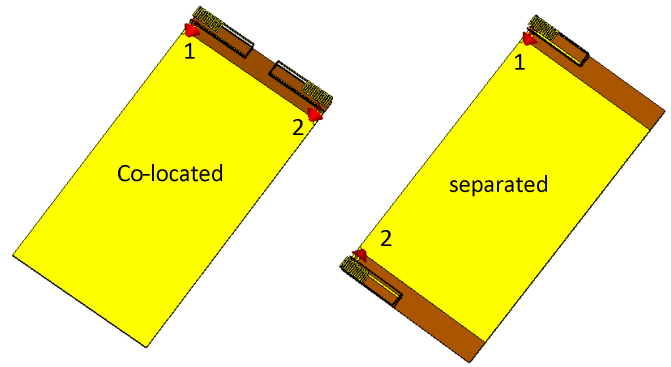

(a) Group A

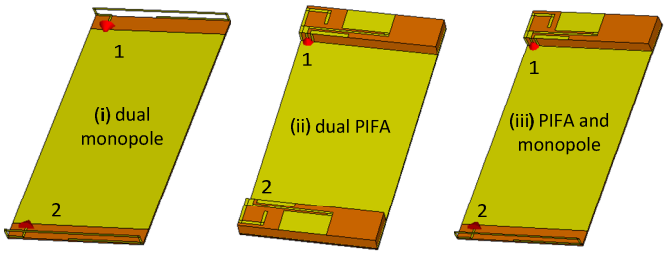

(b) Group B

Fig. 1. Antenna configurations for (a) different antenna locations. (b) different antenna types.

Simulation setup: The simulations were carried out using the time domain solver of CST Microwave Studio. In the simulation, the accepted power at the antennas was set to 24dBm (0.25W) for the low band and 21dBm (0.13W) for the high band. The accepted power is used to represent the worst case SAR, since the antenna mismatch, which can reduce the radiated power and the SAR value, is excluded. In a real life situation, integrated power amplifiers are typically capable of compensating a mismatch by increasing the power delivered to the antennas, hence compensating somehow the antenna detuning. To impose the power constraint of MIMO systems, for stand-alone SAR calculation, all the power was fed into one port, with the other port loaded with 50 Ω, whereas the same input power was evenly divided over the two ports for simultaneous SAR calculation. In the tables and figures below, all the SAR values are expressed in peak 1 g spatial-average SAR and represented in 1g SAR distributions.

TABLE I. DIELECTRIC PARAMETERS OF THE FLAT PHANTOM

	Target Frequency [MHz]	**Relative Permittivity ε_r**	**Conductivity σ [S/m]**
Inner liquid	859	41.5	0.926
	1920	40	1.4
Outer Shell	859 & 1920	3.7	0.0016

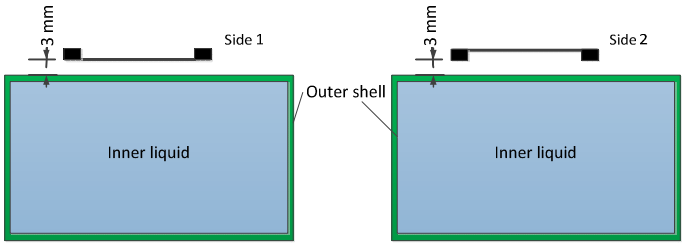

Fig. 2. The flat phantom and the position of the antennas.

III. SAR FOR DIFFERENT ANTENNA LOCATIONS

A. Stand-alone SAR

In this section, the effect of antenna location is analyzed using the antennas in Group A. Stand-alone SAR was simulated with one antenna transmitting and the other antenna loaded with 50 Ω. The simulation results are shown in Fig. 3 (a) and (b) respectively, for the low frequency and high frequency bands. Since the two antennas in each setup are identical to each other and placed in mirror symmetry, the results for only one port are shown.

It is observed that the co-located and separated antenna setups provide similar stand-alone SAR values, though the separation between the antennas differs substantially for the two cases. The reason is as follows: When the coupled monopole is placed on the short edge of the chassis, the chassis is excited as an efficient radiator, which radiates as a dipole along its length [11]. This simultaneous excitation of the chassis induces similar radiation behavior, such as mutual coupling, current distribution and *E* field distribution, for the two setups, resulting in similar SAR values.

The magnitudes of the electric (*E*) field at a plane 12 mm below the chassis for both setups at 0.859 GHz in free space (with Port 1 excited) are presented in Fig. 4, with the solid black frame indicating the position of the mobile handset.

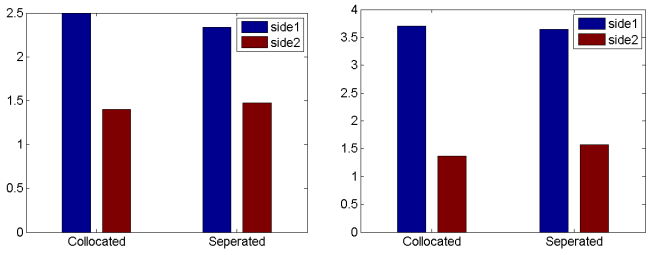

(a) 0.859 GHz (b) 1.92 GHz

Fig. 3. Stand-alone SAR for co-located and separated antenna setups.

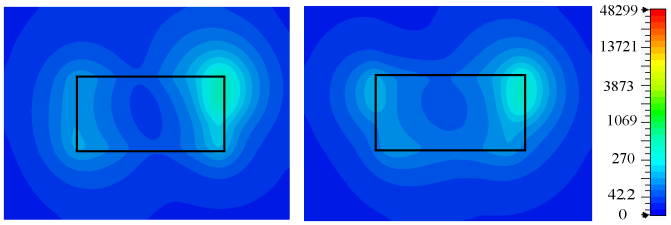

(a) co-located setup (b) separated setup

Fig. 4. Magnitude of *E* field distributions for different antenna setups in free space at 0.859 GHz.

It is seen that the two *E*-field distributions show similar trends even though the antenna locations differ substantially. The *E* field distributions are similar as that for a flat dipole positioned along the chassis length.

Concerning the SAR value for the different sides, the SAR values for side 1 are larger than those for side 2 in each case. This can be attributed to the strong currents on the chassis when the antenna is excited. Moreover, the currents on the antenna elements are stronger on the lower branches, which are printed on the PCB. Thus, when the chassis side (i.e., side 1) is closer to the phantom, the SAR values are higher.

B. Average Simultaneous SAR

Average simultaneous SAR is studied in a similar way as stand-alone SAR. When spatial multiplexing or adaptive beamforming is applied at the multiple antennas, the phase difference between the antenna ports is random. Thus, the simultaneous SAR is averaged over different phase shifts between the ports, and presented in Fig. 5. Compared with stand-alone SAR, average simultaneous SAR always shows a smaller value. The other observation is that the co-located case only shows a slightly higher value of SAR than the separated case when the two antennas are excited simultaneously. This conclusion is quite different from that achieved with SPLSR as a criterion [10]. For SPLSR, where the sum of the stand-alone SAR values is divided by the distance between the hotspots, the co-located antenna setup leads to a much higher value than the separated case. However, if instead the talking mode with hand and head is considered (see Fig. 6), the co-located setup gives lower averaged simultaneous SAR values than the separated setup, since both (co-located) antennas can be placed at the bottom, which corresponds to a larger distance to the head and hence a smaller SAR value. In Fig. 6, one specific hand grip was simulated, and the exact SAR values can change with different hand grips [12].

The SAR distributions in terms of the minimum and maximum SAR values at 0.859 GHz are presented in Table II. For the co-located setup, the minimum SAR is achieved when the phase shift is 0°, whereas the maximum is achieved at a phase shift of 180°. The co-located case shows the opposite behavior with regards to the phase shift. In general, when the SAR distribution is more uniformly spread over the chassis, the minimum SAR value is obtained. On the contrary, the maximum value is a result of a more focused SAR distribution below the antenna elements.

From the perspective of antenna design, the co-located setup can be more convenient for implementation (e.g. requiring only one location and shorter feed cables) and still provide comparable, if not lower, SAR values as the separated antenna setup.

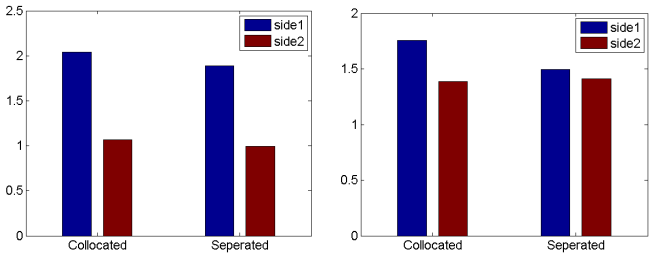

(a) 0.859 GHz (b) 1.92 GHz

Fig. 5. Average simultaneous SAR for co-located and separated antenna setups.

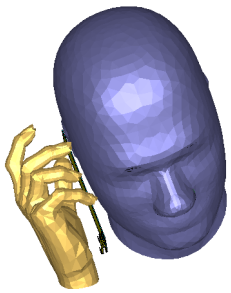

Fig. 6. Mobile handset with hand and head phantom.

TABLE II. SAR DISTRIBUTIONS FOR DIFFERENT PHASE SHIFTS (0.859 GHZ, SIDE 1)

Setup	**Co-located**		**Separated**	
Phase shift	Δφ=0°	Δφ=180°	Δφ=0°	Δφ=180°
1g SAR distribution	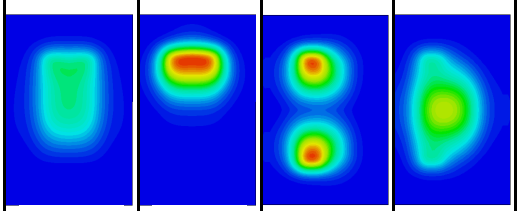			
1g SAR	1.2 W/Kg	2.7 W/Kg	1.8 W/Kg	1.3 W/Kg

IV. SAR For Different Antenna Types

A. Stand-alone SAR

In this section, different antenna types (Group B in Fig. 1) are investigated for SAR performance. The stand-alone SAR for the B(i) monopole setup and the B(ii) PIFA setup are shown in Fig. 7. In general, it is observed that PIFA provides a lower SAR value than monopole, except for the side 2 case at 1.92 GHz. This result can be explained by the more directive radiation of PIFAs (away from the ground plane) as compared to the more omnidirectional radiation of monopoles. The exception is due to the current distributions on the antenna elements, which are important when the antenna elements are facing the phantom. The magnitude of current distributions for the monopole and PIFA are shown in Fig. 8. It is observed that for the monopole, the current at 1.92 GHz is stronger at its lower branch, which is close to the chassis according to Fig.1(b). For the PIFA, the current is focused on the shorter branch on the patch. Thus, when the antennas are facing the flat phantom, the radiation source (current) for the PIFA is closer to the phantom than the monopole, resulting in a higher SAR value.

If different sides are compared, it is seen that side 1 performs better than side 2 in general. For side 1, the current is spread along the chassis, which leads to less-focused hot spots, and lower SAR values. On the contrary, the currents on the antenna elements play a significant role for side 2, resulting in focused hot spots and higher SAR values. The exception of the monopole at 1.92 GHz is also due to its current along the lower folded branch.

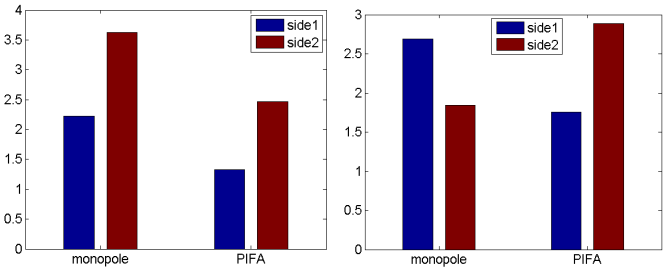

(a) 0.859 GHz (b) 1.92 GHz

Fig. 7. Stand-alone SAR for antenna setups with different antenna types.

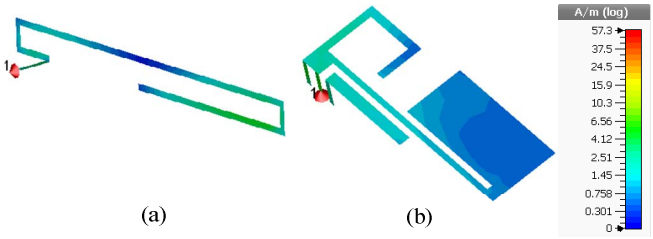

(a) (b)

Fig. 8. Current distribution for monopole and PIFA antennas at 1.92 GHz.

B. Average Simultanious SAR

The average simultaneous SAR values of the two antenna setups are shown in Fig. 9. Compared with the stand-alone SAR, the trend in the performance is similar, though with slightly lower SAR values for each case. If specific SAR values over different phase shifts are considered, for side 1, each SAR value is close to the average value, whereas for side 2 the difference between the minimum and maximum SAR values is larger. This is also because the chassis gives a more uniform SAR distribution, as compared with the more focused distribution provided by the antenna elements when facing the flat phantom.

Since the PIFA provides a lower SAR value than the monopole, if the monopole and PIFA are used together in the mobile handset as in Group B(iii), and considering the talking mode in Fig. 6, it is better to implement the PIFA at the top and the monopole at the bottom, as this strategy should reduce the overall SAR.

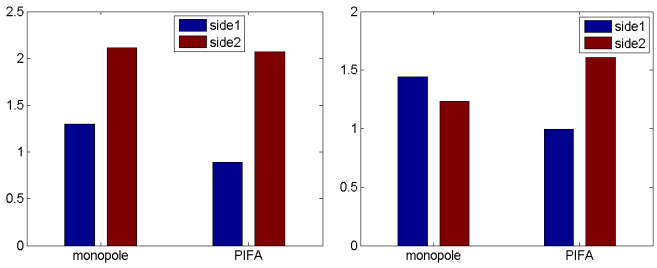

(a) 0.859 GHz (b) 1.92 GHz

Fig. 9. Average simultaneous SAR for antenna setups with different antenna types.

V. Conclusions

In this work, the SAR of dual-antenna mobile handsets for the flat phantom case was evaluated and compared for different antenna locations and types, with the screen or the back side facing the phantom. Both stand-alone SAR and simultaneous SAR were investigated. The results show that stand-alone SAR and average simultaneous SAR give the same trend for SAR values. For antenna location, the co-located and separated antenna setups show a similar behavior; however, considering the talking mode and implementation on PCB, the co-located case may be preferred. For antenna type, the PIFA gives a lower SAR value in general. Nevertheless, in practice, the smaller bandwidth of the PIFA also needs to be taken into account since it may be severely detuned when placed close to the body. The SAR values on different sides depend on the antenna design and current distributions at a specific frequency. Experimental verification of the SAR has been carried out for selective cases system and similar behaviors have been observed. Finally, although the study is based on dual-antenna terminal prototypes, the achieved insights are expected to be valid in general for multi-antenna terminals.

REFERENCES

.

[1] "Human Exposure to Radio Frequency Fields from Handheld and Body-Mounted Wireless Communication Devices – Human Models, Instrumentation, and Procedures – Part 2: Procedure to Determine the Specific Absorption Rate (SAR) in the Head and Body for 30 MHz to 6 GHz Handheld and Body-Mounted Devices Used in Close Proximity to the Ear (Frequency Range of 300 MHz to 3 GHz),"IEC 62209-1, March 2010.

[2] "Human Exposure to Radio Frequency Fields from Handheld and Body-Mounted Wireless Communication Devices – Human Models, Instrumentation, and Procedures – Part 2: Procedure to Determine the Specific Absorption Rate (SAR) in the Head and Body for 30 MHz to 6 GHz Handheld and Body-Mounted Devices Used in Close Proximity to the Ear (Frequency Range of 300 MHz to 3 GHz),"IEC 62209-2, March, 2010.

[3] *IEEE Recommended Practice for Determining the Peak Spatial-Average Specific Absorption Rate (SAR) in the Human Head From Wireless Communications Devices: Measurement Techniques*. IEEE Std. 1528, 2013.

[4] J. Wannstrom. *LTE-Advanced*. Available: http://www.3gpp.org/Technologies/Keywords-Acronyms/LTE-Advanced

[5] O. Kivekas, J. Ollikainen, T. Lehtiniemi, and P. Vainikainen, "Bandwidth, SAR, and efficiency of internal mobile phone antennas," *IEEE Trans. Electromagn. Compat.,* vol. 46, pp. 71-86, Feb 2004.

[6] M. Siegbahn, G. Bit-Babik, J. Keshvari, A. Christ, B. Derat, V. Monebhurrun, C. Penney, M. Vogel, and T. Wittig, "An international interlaboratory comparison of mobile phone SAR calculation with CAD-based models," *IEEE Trans. Electromagn. Compat.,* vol. 52, pp. 804-811, Nov 2010.

[7] C. H. Chang and K. L. Wong, "Printed lambda/8-PIFA for penta-band WWAN operation in the mobile phone," *IEEE Trans. Antennas Propag.,* vol. 57, pp. 1373-1381, May 2009.

[8] N. Perentos, S. Iskra, A. Faraone, R. J. McKenzie, G. Bit-Babik, and V. Anderson, "Exposure compliance methodologies for multiple input multiple output (MIMO) enabled networks and terminals," *IEEE Trans. Antennas Propag.,* vol. 60, pp. 644-653, Feb 2012.

[9] M. S. Wang, L. Lin, J. Chen, D. Jackson, W. Kainz, Y. H. Qi, and P. Jarmuszewski, "Evaluation and optimization of the specific absorption rate for multiantenna systems," *IEEE Trans. Electromagn. Compat.,* vol. 53, pp. 628-637, Aug 2011.

[10] K. Zhao, S. Zhang, Z. Ying, T. Bolin, and S. He, "SAR study of different MIMO antena designs for LTE application in smart mobile handsets " *IEEE Trans. Antennas Propag.,* vol. 61, pp. 3270-3279, June 2013.

[11] H. Li, Y. Tan, B. K. Lau, Z. Ying, and S. He, "Characteristic mode based tradeoff analysis of antenna-chassis interactions for multiple antenna terminals," *IEEE Trans. Antennas Propag.,* vol. 60, pp. 490-502, Feb. 2012.

[12] C. H. Li, M. Douglas, E. Ofli, B. Derat, S. Gabriel, N. Chavannes, and N. Kuster, "Influence of the hand on the specific absorption rate in the head," *IEEE Trans. Antennas Propag.,* vol. 60, pp. 1066-1074, Feb 2012.